Measurements of weak decay asymmetries of $\Lambda_c^+ \to pK_s^0$, $\Lambda\pi^+$, $\Sigma^+\pi^0$, and $\Sigma^0\pi^+$

M. Ablikim,[1] M. N. Achasov,[10,d] P. Adlarson,[58] S. Ahmed,[15] M. Albrecht,[4] M. Alekseev,[57a,57c] A. Amoroso,[57a,57c] F. F. An,[1] Q. An,[54,42] Y. Bai,[41] O. Bakina,[27] R. Baldini Ferroli,[23a] Y. Ban,[35] K. Begzsuren,[25] J. V. Bennett,[5] N. Berger,[26] M. Bertani,[23a] D. Bettoni,[24a] F. Bianchi,[57a,57c] J. Biernat,[58] J. Bloms,[51] I. Boyko,[27] R. A. Briere,[5] H. Cai,[59] X. Cai,[1,42] A. Calcaterra,[23a] G. F. Cao,[1,46] N. Cao,[1,46] S. A. Cetin,[45b] J. Chai,[57c] J. F. Chang,[1,42] W. L. Chang,[1,46] G. Chelkov,[27,b,c] D. Y. Chen,[6] G. Chen,[1] H. S. Chen,[1,46] J. C. Chen,[1] M. L. Chen,[1,42] S. J. Chen,[33] Y. B. Chen,[1,42] W. Cheng,[57c] G. Cibinetto,[24a] F. Cossio,[57c] X. F. Cui,[34] H. L. Dai,[1,42] J. P. Dai,[37,h] X. C. Dai,[1,46] A. Dbeyssi,[15] D. Dedovich,[27] Z. Y. Deng,[1] A. Denig,[26] I. Denysenko,[27] M. Destefanis,[57a,57c] F. De Mori,[57a,57c] Y. Ding,[31] C. Dong,[34] J. Dong,[1,42] L. Y. Dong,[1,46] M. Y. Dong,[1,42,46] Z. L. Dou,[33] S. X. Du,[62] J. Z. Fan,[44] J. Fang,[1,42] S. S. Fang,[1,46] Y. Fang,[1] R. Farinelli,[24a,24b] L. Fava,[57b,57c] F. Feldbauer,[4] G. Felici,[23a] C. Q. Feng,[54,42] M. Fritsch,[4] C. D. Fu,[1] Y. Fu,[1] Q. Gao,[1] X. L. Gao,[54,42] Y. Gao,[55] Y. Gao,[44] Y. G. Gao,[6] Z. Gao,[54,42] B. Garillon,[26] I. Garzia,[24a] E. M. Gersabeck,[49] A. Gilman,[50] K. Goetzen,[11] L. Gong,[34] W. X. Gong,[1,42] W. Gradl,[26] M. Greco,[57a,57c] L. M. Gu,[33] M. H. Gu,[1,42] S. Gu Gu,[2] Y. T. Gu,[13] A. Q. Guo,[22] L. B. Guo,[32] R. P. Guo,[1,46] Y. P. Guo,[26] A. Guskov,[27] S. Han,[59] X. Q. Hao,[16] F. A. Harris,[47] K. L. He,[1,46] F. H. Heinsius,[4] T. Held,[4] Y. K. Heng,[1,42,46] Y. R. Hou,[46] Z. L. Hou,[1] H. M. Hu,[1,46] J. F. Hu,[37,h] T. Hu,[1,42,46] Y. Hu,[1] G. S. Huang,[54,42] J. S. Huang,[16] X. T. Huang,[36] X. Z. Huang,[33] Z. L. Huang,[31] N. Huesken,[51] T. Hussain,[56] W. Ikegami Andersson,[58] W. Imoehl,[22] M. Irshad,[54,42] Q. Ji,[1] Q. P. Ji,[16] X. B. Ji,[1,46] X. L. Ji,[1,42] H. L. Jiang,[36] X. S. Jiang,[1,42,46] X. Y. Jiang,[34] J. B. Jiao,[36] Z. Jiao,[18] D. P. Jin,[1,42,46] S. Jin,[33] Y. Jin,[48] T. Johansson,[58] N. Kalantar-Nayestanaki,[29] X. S. Kang,[31] R. Kappert,[29] M. Kavatsyuk,[29] B. C. Ke,[1] I. K. Keshk,[4] T. Khan,[54,42] A. Khoukaz,[51] P. Kiese,[26] R. Kiuchi,[1] R. Kliemt,[11] L. Koch,[28] O. B. Kolcu,[45b,f] B. Kopf,[4] M. Kuemmel,[4] M. Kuessner,[4] A. Kupsc,[58] M. Kurth,[1] M. G. Kurth,[1,46] W. Kühn,[28] J. S. Lange,[28] P. Larin,[15] L. Lavezzi,[57c] H. Leithoff,[26] T. Lenz,[26] C. Li,[58] Cheng Li,[54,42] D. M. Li,[62] F. Li,[1,42] F. Y. Li,[35] G. Li,[1] H. B. Li,[1,46] H. J. Li,[9,j] J. C. Li,[1] J. W. Li,[40] Ke Li,[1] L. K. Li,[1] Lei Li,[3] P. L. Li,[54,42] P. R. Li,[30] Q. Y. Li,[36] W. D. Li,[1,46] W. G. Li,[1] X. H. Li,[54,42] X. L. Li,[36] X. N. Li,[1,42] X. Q. Li,[34] Z. B. Li,[43] Z. Y. Li,[43] H. Liang,[1,46] H. Liang,[54,42] Y. F. Liang,[39] Y. T. Liang,[28] G. R. Liao,[12] L. Z. Liao,[1,46] J. Libby,[21] C. X. Lin,[43] D. X. Lin,[15] Y. J. Lin,[13] B. Liu,[37,h] B. J. Liu,[1] C. X. Liu,[1] D. Liu,[54,42] D. Y. Liu,[37,h] F. H. Liu,[38] Fang Liu,[1] Feng Liu,[6] H. B. Liu,[13] H. M. Liu,[1,46] Huanhuan Liu,[1] Huihui Liu,[17] J. B. Liu,[54,42] J. Y. Liu,[1,46] K. Y. Liu,[31] Ke Liu,[6] Q. Liu,[46] S. B. Liu,[54,42] T. Liu,[1,46] X. Liu,[30] X. Y. Liu,[1,46] Y. B. Liu,[34] Z. A. Liu,[1,42,46] Zhiqing Liu,[26] Y. F. Long,[35] X. C. Lou,[1,42,46] H. J. Lu,[18] J. D. Lu,[1,46] J. G. Lu,[1,42] Y. Lu,[1] Y. P. Lu,[1,42] C. L. Luo,[32] M. X. Luo,[61] P. W. Luo,[43] T. Luo,[9,j] X. L. Luo,[1,42] S. Lusso,[57c] X. R. Lyu,[46] F. C. Ma,[31] H. L. Ma,[1] L. L. Ma,[36] M. M. Ma,[1,46] Q. M. Ma,[1] X. N. Ma,[34] X. X. Ma,[1,46] X. Y. Ma,[1,42] Y. M. Ma,[36] F. E. Maas,[15] M. Maggiora,[57a,57c] S. Maldaner,[26] S. Malde,[52] Q. A. Malik,[56] A. Mangoni,[23b] Y. J. Mao,[35] Z. P. Mao,[1] S. Marcello,[57a,57c] Z. X. Meng,[48] J. G. Messchendorp,[29] G. Mezzadri,[24a] J. Min,[1,42] T. J. Min,[33] R. E. Mitchell,[22] X. H. Mo,[1,42,46] Y. J. Mo,[6] C. Morales Morales,[15] N. Yu. Muchnoi,[10,d] H. Muramatsu,[50] A. Mustafa,[4] S. Nakhoul,[11,g] Y. Nefedov,[27] F. Nerling,[11,g] I. B. Nikolaev,[10,d] Z. Ning,[1,42] S. Nisar,[8,k] S. L. Niu,[1,42] S. L. Olsen,[46] Q. Ouyang,[1,42,46] S. Pacetti,[23b] Y. Pan,[54,42] M. Papenbrock,[58] P. Patteri,[23a] M. Pelizaeus,[4] H. P. Peng,[54,42] K. Peters,[11,g] J. Pettersson,[58] J. L. Ping,[32] R. G. Ping,[1,46] A. Pitka,[4] R. Poling,[50] V. Prasad,[54,42] M. Qi,[33] T. Y. Qi,[2] S. Qian,[1,42] C. F. Qiao,[46] N. Qin,[59] X. P. Qin,[13] X. S. Qin,[4] Z. H. Qin,[1,42] J. F. Qiu,[1] S. Q. Qu,[34] K. H. Rashid,[56,i] C. F. Redmer,[26] M. Richter,[4] M. Ripka,[26] A. Rivetti,[57c] V. Rodin,[29] M. Rolo,[57c] G. Rong,[1,46] Ch. Rosner,[15] M. Rump,[51] A. Sarantsev,[27,e] M. Savrié,[24b] K. Schoenning,[58] W. Shan,[19] X. Y. Shan,[54,42] M. Shao,[54,42] C. P. Shen,[2] P. X. Shen,[34] X. Y. Shen,[1,46] H. Y. Sheng,[1] X. Shi,[1,42] X. D. Shi,[54,42] J. J. Song,[36] Q. Q. Song,[54,42] X. Y. Song,[1] S. Sosio,[57a,57c] C. Sowa,[4] S. Spataro,[57a,57c] F. F. Sui,[36] G. X. Sun,[1] J. F. Sun,[16] L. Sun,[59] S. S. Sun,[1,46] X. H. Sun,[1] Y. J. Sun,[54,42] Y. K. Sun,[54,42] Y. Z. Sun,[1] Z. J. Sun,[1,42] Z. T. Sun,[1] Y. T. Tan,[54,42] C. J. Tang,[39] G. Y. Tang,[1] X. Tang,[1] V. Thoren,[58] B. Tsednee,[25] I. Uman,[45d] B. Wang,[1] B. L. Wang,[46] C. W. Wang,[33] D. Y. Wang,[35] H. H. Wang,[36] K. Wang,[1,42] L. L. Wang,[1] L. S. Wang,[1] M. Wang,[36] M. Z. Wang,[35] Meng Wang,[1,46] P. L. Wang,[1] R. M. Wang,[60] W. P. Wang,[54,42] X. Wang,[35] X. F. Wang,[1] X. L. Wang,[9,j] Y. Wang,[54,42] Y. Wang,[43] Y. F. Wang,[1,42,46] Z. Wang,[1,42] Z. G. Wang,[1,42] Z. Y. Wang,[1] Zongyuan Wang,[1,46] T. Weber,[4] D. H. Wei,[12] P. Weidenkaff,[26] H. W. Wen,[32] S. P. Wen,[1] U. Wiedner,[4] G. Wilkinson,[52] M. Wolke,[58] L. H. Wu,[1] L. J. Wu,[1,46] Z. Wu,[1,42] L. Xia,[54,42] Y. Xia,[20] S. Y. Xiao,[1] Y. J. Xiao,[1,46] Z. J. Xiao,[32] Y. G. Xie,[1,42] Y. H. Xie,[6] T. Y. Xing,[1,46] X. A. Xiong,[1,46] Q. L. Xiu,[1,42] G. F. Xu,[1] L. Xu,[1] Q. J. Xu,[14] W. Xu,[1,46] X. P. Xu,[40] F. Yan,[55] L. Yan,[57a,57c] W. B. Yan,[54,42] W. C. Yan,[2] Y. H. Yan,[20] H. J. Yang,[37,h] H. X. Yang,[1] L. Yang,[59] R. X. Yang,[54,42] S. L. Yang,[1,46] Y. H. Yang,[33] Y. X. Yang,[12] Yifan Yang,[1,46] Z. Q. Yang,[20] M. Ye,[1,42] M. H. Ye,[7] J. H. Yin,[1] Z. Y. You,[43] B. X. Yu,[1,42,46] C. X. Yu,[34] J. S. Yu,[20] C. Z. Yuan,[1,46] X. Q. Yuan,[35] Y. Yuan,[1] A. Yuncu,[45b,a] A. A. Zafar,[56] Y. Zeng,[20] B. X. Zhang,[1] B. Y. Zhang,[1,42] C. C. Zhang,[1] D. H. Zhang,[1] H. H. Zhang,[43] H. Y. Zhang,[1,42] J. Zhang,[1,46] J. L. Zhang,[60] J. Q. Zhang,[4] J. W. Zhang,[1,42,46] J. Y. Zhang,[1] J. Z. Zhang,[1,46] K. Zhang,[1,46] L. Zhang,[44] S. F. Zhang,[33] T. J. Zhang,[37,h] X. Y. Zhang,[36] Y. Zhang,[54,42] Y. H. Zhang,[1,42] Y. T. Zhang,[54,42] Yang Zhang,[1] Yao Zhang,[1] Yi Zhang,[9,j] Yu Zhang,[46] Z. H. Zhang,[6] Z. P. Zhang,[54] Z. Y. Zhang,[59] G. Zhao,[1]

J. W. Zhao,[1,42] J. Y. Zhao,[1,46] J. Z. Zhao,[1,42] Lei Zhao,[54,42] Ling Zhao,[1] M. G. Zhao,[34] Q. Zhao,[1] S. J. Zhao,[62] T. C. Zhao,[1] Y. B. Zhao,[1,42] Z. G. Zhao,[54,42] A. Zhemchugov,[27,b] B. Zheng,[55] J. P. Zheng,[1,42] Y. Zheng,[35] Y. H. Zheng,[46] B. Zhong,[32] L. Zhou,[1,42] L. P. Zhou,[1,46] Q. Zhou,[1,46] X. Zhou,[59] X. K. Zhou,[46] X. R. Zhou,[54,42] Xiaoyu Zhou,[20] Xu Zhou,[20] A. N. Zhu,[1,46] J. Zhu,[34] J. Zhu,[43] K. Zhu,[1] K. J. Zhu,[1,42,46] S. H. Zhu,[53] W. J. Zhu,[34] X. L. Zhu,[44] Y. C. Zhu,[54,42] Y. S. Zhu,[1,46] Z. A. Zhu,[1,46] J. Zhuang,[1,42] B. S. Zou,[1] and J. H. Zou[1]

(BESIII Collaboration)

[1]*Institute of High Energy Physics, Beijing 100049, People's Republic of China*
[2]*Beihang University, Beijing 100191, People's Republic of China*
[3]*Beijing Institute of Petrochemical Technology, Beijing 102617, People's Republic of China*
[4]*Bochum Ruhr-University, D-44780 Bochum, Germany*
[5]*Carnegie Mellon University, Pittsburgh, Pennsylvania 15213, USA*
[6]*Central China Normal University, Wuhan 430079, People's Republic of China*
[7]*China Center of Advanced Science and Technology, Beijing 100190, People's Republic of China*
[8]*COMSATS University Islamabad, Lahore Campus, Defence Road, Off Raiwind Road, 54000 Lahore, Pakistan*
[9]*Fudan University, Shanghai 200443, People's Republic of China*
[10]*G.I. Budker Institute of Nuclear Physics SB RAS (BINP), Novosibirsk 630090, Russia*
[11]*GSI Helmholtzcentre for Heavy Ion Research GmbH, D-64291 Darmstadt, Germany*
[12]*Guangxi Normal University, Guilin 541004, People's Republic of China*
[13]*Guangxi University, Nanning 530004, People's Republic of China*
[14]*Hangzhou Normal University, Hangzhou 310036, People's Republic of China*
[15]*Helmholtz Institute Mainz, Johann-Joachim-Becher-Weg 45, D-55099 Mainz, Germany*
[16]*Henan Normal University, Xinxiang 453007, People's Republic of China*
[17]*Henan University of Science and Technology, Luoyang 471003, People's Republic of China*
[18]*Huangshan College, Huangshan 245000, People's Republic of China*
[19]*Hunan Normal University, Changsha 410081, People's Republic of China*
[20]*Hunan University, Changsha 410082, People's Republic of China*
[21]*Indian Institute of Technology Madras, Chennai 600036, India*
[22]*Indiana University, Bloomington, Indiana 47405, USA*
[23a]*INFN Laboratori Nazionali di Frascati, I-00044 Frascati, Italy*
[23b]*INFN and University of Perugia, I-06100 Perugia, Italy*
[24a]*INFN Sezione di Ferrara, I-44122 Ferrara, Italy*
[24b]*University of Ferrara, I-44122 Ferrara, Italy*
[25]*Institute of Physics and Technology, Peace Avenue 54B, Ulaanbaatar 13330, Mongolia*
[26]*Johannes Gutenberg University of Mainz, Johann-Joachim-Becher-Weg 45, D-55099 Mainz, Germany*
[27]*Joint Institute for Nuclear Research, 141980 Dubna, Moscow region, Russia*
[28]*Justus-Liebig-Universitaet Giessen, II. Physikalisches Institut, Heinrich-Buff-Ring 16, D-35392 Giessen, Germany*
[29]*KVI-CART, University of Groningen, NL-9747 AA Groningen, Netherlands*
[30]*Lanzhou University, Lanzhou 730000, People's Republic of China*
[31]*Liaoning University, Shenyang 110036, People's Republic of China*
[32]*Nanjing Normal University, Nanjing 210023, People's Republic of China*
[33]*Nanjing University, Nanjing 210093, People's Republic of China*
[34]*Nankai University, Tianjin 300071, People's Republic of China*
[35]*Peking University, Beijing 100871, People's Republic of China*
[36]*Shandong University, Jinan 250100, People's Republic of China*
[37]*Shanghai Jiao Tong University, Shanghai 200240, People's Republic of China*
[38]*Shanxi University, Taiyuan 030006, People's Republic of China*
[39]*Sichuan University, Chengdu 610064, People's Republic of China*
[40]*Soochow University, Suzhou 215006, People's Republic of China*
[41]*Southeast University, Nanjing 211100, People's Republic of China*
[42]*State Key Laboratory of Particle Detection and Electronics, Beijing 100049, Hefei 230026, People's Republic of China*
[43]*Sun Yat-Sen University, Guangzhou 510275, People's Republic of China*
[44]*Tsinghua University, Beijing 100084, People's Republic of China*
[45a]*Ankara University, 06100 Tandogan, Ankara, Turkey*
[45b]*Istanbul Bilgi University, 34060 Eyup, Istanbul, Turkey*
[45c]*Uludag University, 16059 Bursa, Turkey*
[45d]*Near East University, Nicosia, North Cyprus, Mersin 10, Turkey*

[46]University of Chinese Academy of Sciences, Beijing 100049, People's Republic of China
[47]University of Hawaii, Honolulu, Hawaii 96822, USA
[48]University of Jinan, Jinan 250022, People's Republic of China
[49]University of Manchester, Oxford Road, Manchester, M13 9PL, United Kingdom
[50]University of Minnesota, Minneapolis, Minnesota 55455, USA
[51]University of Muenster, Wilhelm-Klemm-Str. 9, 48149 Muenster, Germany
[52]University of Oxford, Keble Rd, Oxford OX13RH, United Kingdom
[53]University of Science and Technology Liaoning, Anshan 114051, People's Republic of China
[54]University of Science and Technology of China, Hefei 230026, People's Republic of China
[55]University of South China, Hengyang 421001, People's Republic of China
[56]University of the Punjab, Lahore-54590, Pakistan
[57a]University of Turin, I-10125 Turin, Italy
[57b]University of Eastern Piedmont, I-15121 Alessandria, Italy
[57c]INFN, I-10125 Turin, Italy
[58]Uppsala University, Box 516, SE-75120 Uppsala, Sweden
[59]Wuhan University, Wuhan 430072, People's Republic of China
[60]Xinyang Normal University, Xinyang 464000, People's Republic of China
[61]Zhejiang University, Hangzhou 310027, People's Republic of China
[62]Zhengzhou University, Zhengzhou 450001, People's Republic of China

(Received 10 May 2019; published 14 October 2019)

Using $e^+e^- \to \Lambda_c^+ \bar{\Lambda}_c^-$ production from a 567 pb^{-1} data sample collected by BESIII at 4.6 GeV, a full angular analysis is carried out simultaneously on the four decay modes of $\Lambda_c^+ \to pK_S^0$, $\Lambda\pi^+$, $\Sigma^+\pi^0$, and $\Sigma^0\pi^+$. For the first time, the Λ_c^+ transverse polarization is studied in unpolarized e^+e^- collisions, where a nonzero effect is observed with a statistical significance of 2.1σ. The decay asymmetry parameters of the Λ_c^+ weak hadronic decays into pK_S^0, $\Lambda\pi^+$, $\Sigma^+\pi^0$ and $\Sigma^0\pi^+$ are measured to be $0.18 \pm 0.43(\text{stat}) \pm 0.14(\text{syst})$, $-0.80 \pm 0.11(\text{stat}) \pm 0.02(\text{syst})$, $-0.57 \pm 0.10(\text{stat}) \pm 0.07(\text{syst})$, and $-0.73 \pm 0.17(\text{stat}) \pm 0.07(\text{syst})$, respectively. In comparison with previous results, the measurements for the $\Lambda\pi^+$ and $\Sigma^+\pi^0$ modes are consistent but with improved precision, while the parameters for the pK_S^0 and $\Sigma^0\pi^+$ modes are measured for the first time.

DOI: 10.1103/PhysRevD.100.072004

[a]Also at Bogazici University, 34342 Istanbul, Turkey.
[b]Also at the Moscow Institute of Physics and Technology, Moscow 141700, Russia.
[c]Also at the Functional Electronics Laboratory, Tomsk State University, Tomsk 634050, Russia.
[d]Also at the Novosibirsk State University, Novosibirsk 630090, Russia.
[e]Also at the NRC "Kurchatov Institute", PNPI, 188300 Gatchina, Russia.
[f]Also at Istanbul Arel University, 34295 Istanbul, Turkey.
[g]Also at Goethe University Frankfurt, 60323 Frankfurt am Main, Germany.
[h]Also at Key Laboratory for Particle Physics, Astrophysics and Cosmology, Ministry of Education; Shanghai Key Laboratory for Particle Physics and Cosmology; Institute of Nuclear and Particle Physics, Shanghai 200240, People's Republic of China.
[i]Also at Government College Women University, Sialkot—51310 Punjab, Pakistan.
[j]Also at Key Laboratory of Nuclear Physics and Ion-beam Application (MOE) and Institute of Modern Physics, Fudan University, Shanghai 200443, People's Republic of China.
[k]Also at Harvard University, Department of Physics, Cambridge, Massachusetts 02138, USA.

I. INTRODUCTION

The study of the lightest charmed baryon Λ_c^+ is important for the understanding of the whole charmed baryon sector. In recent years, there has been significant progress in studying the Λ_c^+, both experimentally and theoretically [1,2]. This provides crucial information in detailed explorations of the singly charmed baryons (Σ_c, Ξ_c and Ω_c) [3,4], and further searches or discoveries of the doubly charmed baryons (Ξ_{cc} and Ω_{cc}) [5,6]. Moreover, as the charmed baryon is the favored weak decay final state of b-baryons and its properties are inputs to study b-baryons, improved knowledge in the charm sector can contribute substantially to understanding the properties of b-baryons.

Some QCD-inspired charmed baryon models that have been developed [7] are the flavor symmetry model [8], factorization model [9], pole model [10], and current algebra framework [11]. As shown in Refs. [2,7], many of these models calculate Λ_c^+ decay rates in good agreement with experimental results. But the decay asymmetries predicted by these models for Λ_c^+ two-body hadronic weak decays do not agree very well.

The decay asymmetry parameter, α_{BP}^+, in a weak decay $\Lambda_c^+ \to BP$ (B denotes a $J^P = \frac{1}{2}^+$ baryon and P denotes a

$J^P = 0^-$ pseudoscalar meson) is defined as $\alpha^+_{BP} \equiv \frac{2\mathrm{Re}(s^* p)}{|s|^2+|p|^2}$, where s and p stand for the parity-violating s-wave and parity-conserving p-wave amplitudes in the decay, respectively. Model calculations of α^+_{BP} in $\Lambda_c^+ \to pK^0_S$, $\Lambda\pi^+$, $\Sigma^+\pi^0$, and $\Sigma^0\pi^+$ are quite uncertain, with $\alpha^+_{pK^0_S}$ in the range $(-1.0, -0.49)$, $\alpha^+_{\Lambda\pi^+}$ in $(-0.99, -0.67)$, $\alpha^+_{\Sigma^+\pi^0}$ in $(-0.76, -0.31)$ or $(0.39, 0.83)$, and $\alpha^+_{\Sigma^0\pi^+}$ in $(-0.76, -0.31)$ or $(0.43, 0.92)$ [10–18].

As predictions of α^+_{BP} rely on the relative phase between the two amplitudes, the experimental measurements of the decay asymmetry parameters serve as very sensitive probes to test different theoretical models.

Experimentally, only $\alpha^+_{\Lambda\pi^+}$ and $\alpha^+_{\Sigma^+\pi^0}$ have been measured previously [19–22]. The measured value for $\alpha^+_{\Sigma^+\pi^0}$ is -0.45 ± 0.32, in contradiction with the predicted values in many theoretical models [10–15]. Therefore, it is important to carry out independent measurements of $\alpha^+_{\Sigma^+\pi^0}$ to confirm the sign of $\alpha^+_{\Sigma^+\pi^0}$ and test these models. Moreover, $\alpha^+_{\Sigma^+\pi^0}$ and $\alpha^+_{\Sigma^0\pi^+}$ should have the same value according to hyperon isospin symmetry [16], and any deviation from this expectation provides critical information on final state interactions in Λ_c^+ hadronic decays. All these models predict $\alpha^+_{\Lambda\pi^+}$ consistent with the measured values, and it is necessary to further improve the experimental precision to discriminate between them.

In previous experiments, Λ_c^+ was assumed to be unpolarized, and the decay asymmetry parameter α^+_{BP} was obtained by analyzing the longitudinal polarization from the weak two-body decay of the produced baryon B, such as $\Lambda \to p\pi^-$ and $\Sigma^+ \to p\pi^0$ for $\alpha^+_{\Lambda\pi^+}$ and $\alpha^+_{\Sigma^+\pi^0}$, respectively. However, the hypothesis of unpolarized Λ_c^+ may not be valid. There have been observations of transverse Λ polarization in inclusive Λ production in e^+e^- collisions at 10.58 GeV [23] and in $e^+e^- \to \Lambda\bar{\Lambda}$ at J/ψ mass position [24], and it has been postulated that the produced Λ_c^+ could be polarized [25]. Further, as the polarization of the proton in the decay $\Lambda_c^+ \to pK^0_S$ is not accessible with the above method, a nonzero transverse polarization of the Λ_c^+ provides an alternative way to measure $\alpha^+_{pK^0_S}$ [26].

In this work, we investigate for the first time the transverse polarization of the Λ_c^+ baryon in unpolarized e^+e^- annihilations. We present for the first time measurements of the decay asymmetry parameters in Λ_c^+ decays into pK^0_S, $\Lambda\pi^+$, $\Sigma^+\pi^0$, and $\Sigma^0\pi^+$ based on a multidimensional angular analysis of the cascade-decay final states, which greatly improves the resulting precision. The data sample used in this analysis corresponds to an integrated luminosity of 567 pb^{-1} collected with the BESIII detector at BEPCII at center-of-mass (CM) energy of 4.6 GeV.

Since the close proximity of the CM energy to the $\Lambda_c^+\bar{\Lambda}_c^-$ mass threshold does not allow an additional hadron to be produced, $\Lambda_c^+\bar{\Lambda}_c^-$ are always generated in pairs, which provides a clean environment to study their decays. When one Λ_c^+ is detected, another $\bar{\Lambda}_c^-$ partner is inferred. Hence, to increase signal yields, we adopt a partial reconstruction method, in which only one Λ_c^+ is reconstructed out of all the final-state particles in an event. The charge conjugation modes are incorporated in the analysis, and they are always implied in the context, unless otherwise stated explicitly.

II. DATA ANALYSIS

Details of the BESIII apparatus, the software framework and the Monte Carlo (MC) simulation sample have been given in Ref. [27]. The Λ_c^+ signal candidates are reconstructed through the decays into pK^0_S, $\Lambda\pi^+$, $\Sigma^+\pi^0$ and $\Sigma^0\pi^+$. Here, the intermediate particles K^0_S, Λ, Σ^+, Σ^0 and π^0 are reconstructed via the decays $K^0_S \to \pi^+\pi^-$, $\Lambda \to p\pi^-$, $\Sigma^+ \to p\pi^0$, $\Sigma^0 \to \gamma\Lambda$, and $\pi^0 \to \gamma\gamma$. The event selection criteria follow those described in Ref. [27], unless otherwise stated explicitly. To suppress the $\Lambda_c^+ \to pK^0_S$, $K^0_S \to \pi^0\pi^0$ events in the $\Sigma^+\pi^0$ candidate samples, the invariant mass of the $\pi^0\pi^0$ system is required to be outside the range $[400, 550]$ MeV/c^2.

For each signal decay mode, the yields are obtained from a fit to the beam-constrained mass (M_{BC}) distribution, $M_{\mathrm{BC}} \equiv \sqrt{E^2_{\mathrm{beam}} - p^2_{\Lambda_c^+}}$, where E_{beam} is the average beam energy and $p_{\Lambda_c^+}$ is the measured Λ_c^+ momentum in the CM system of the e^+e^- collisions. If more than one candidate is reconstructed in the event, the one with the smallest energy

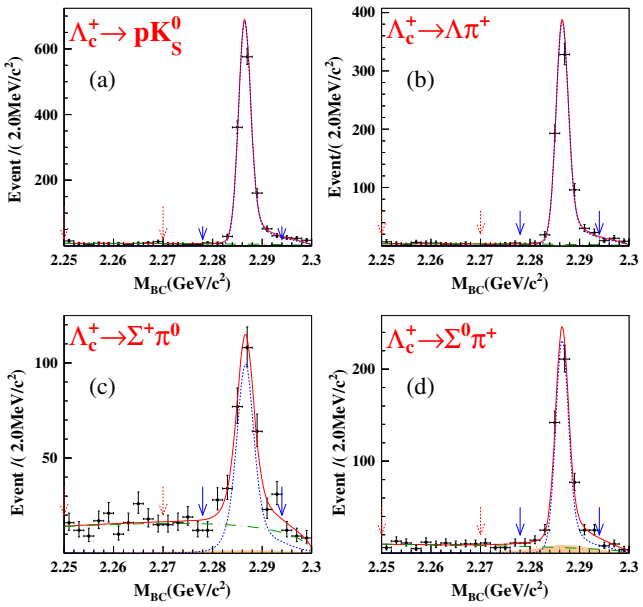

FIG. 1. Fits to the M_{BC} spectra of the signal candidates of (a) $\Lambda_c^+ \to pK^0_S$, (b) $\Lambda_c^+ \to \Lambda\pi^+$, (c) $\Lambda_c^+ \to \Sigma^+\pi^0$, and (d) $\Lambda_c^+ \to \Sigma^0\pi^+$. Points with error bars correspond to data, solid lines are the fitting curves, dashed lines describe the signal events distribution, dash-dotted lines show the Type-II backgrounds and shadowed areas correspond to Type-I backgrounds. Dashed and solid arrows show the sideband and signal regions, respectively.

difference ($|\Delta E|$) is kept, where $\Delta E \equiv E_{\Lambda_c^+} - E_{\rm beam}$, and $E_{\Lambda_c^+}$ is the measured total energy of the Λ_c^+ candidate.

Figure 1 shows the $M_{\rm BC}$ distributions for the signal candidates, where the Λ_c^+ signal peak is evident at the nominal Λ_c^+ mass. The backgrounds can be classified into two types. The Type-I backgrounds are from the true Λ_c^+ signal decays, where at least one of the final state particle candidates is wrongly assigned in reconstruction. The Type-II backgrounds correspond to combinatorial backgrounds mostly from $e^+e^- \to q\bar{q}(q = u, d, s)$ processes. To evaluate the Type-I and Type-II background level, unbinned maximum likelihood fits (shown in Fig. 1) are applied to the $M_{\rm BC}$ spectra. The signal and Type-I background shapes, as well as the ratio of their yields, are derived from the signal MC simulation samples. These two shapes are convolved with a common Gaussian function, whose width is left free and represents the difference in resolution between data and MC simulations. The type-II background shape is modeled by an ARGUS function [28]. The Λ_c^+ signal and sideband regions are chosen as $[2.278, 2.294]$ GeV/c^2 and $[2.250, 2.270]$ GeV/c^2, respectively.

III. DECAY ASYMMETRIES MEASUREMENT

The decay asymmetry parameters are determined by analyzing the multi-dimensional angular distributions, where the full cascade decay chains are considered. The full angular dependence formulas (4), (6), and (10) in Ref. [26], constructed under the helicity basis, are used in the fit. To illustrate the helicity system defined in this analysis, we take as an example the two-level cascade decay process $\Lambda_c^+ \to \Lambda\pi^+$, $\Lambda \to p\pi^-$ following the level-0 process $e^+e^- \to \gamma^* \to \Lambda_c^+\bar{\Lambda}_c^-$. An analogous formalism is applied to the other $\Lambda_c^+ \to BP$ decays.

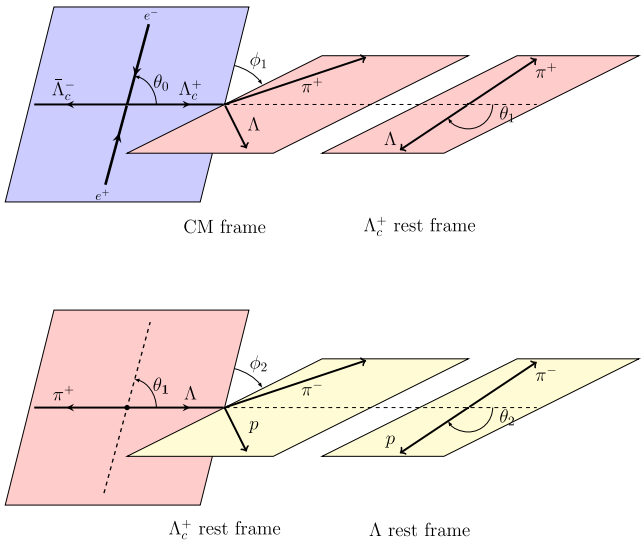

FIG. 2. Definition of the helicity frame for $e^+e^- \to \Lambda_c^+\bar{\Lambda}_c^-$, $\Lambda_c^+ \to \Lambda\pi^+$, $\Lambda \to p\pi^-$.

Figure 2 illustrates the definitions of the full system of helicity angles for the $\Lambda_c^+ \to \Lambda\pi^+$ mode. In the helicity frame of $e^+e^- \to \Lambda_c^+\bar{\Lambda}_c^-$, θ_0 is the polar angle of the Λ_c^+ with respect to the e^+ beam axis in the e^+e^- CM system. For the helicity angles of the $\Lambda_c^+ \to \Lambda\pi^+$ decay, ϕ_1 is the angle between the $e^+\Lambda_c^+$ and $\Lambda\pi^+$ planes, and θ_1 is the polar angle of the Λ momentum in the rest frame of the Λ_c^+ with respect to the Λ_c^+ momentum in the CM frame. The angle subscript represents the level numbering of the cascade signal decays. For the helicity angles describing the $\Lambda \to p\pi^+$ decay, ϕ_2 is the angle between the $\Lambda\pi^+$ plane and $p\pi^-$ plane and θ_2 is the polar angle of the proton momentum with respect to opposite direction of π^+ momentum in the rest frame of Λ. For the three-level cascade decays $\Lambda_c^+ \to \Sigma^0\pi^+$, $\Sigma^0 \to \Lambda\gamma$, $\Lambda \to p\pi^-$ process, ϕ_3 is the angle between the $\Lambda\gamma$ and $p\pi^-$ planes, while θ_3 is the polar angle of the proton with respect to the opposite direction of the photon momentum (from $\Sigma^0 \to \Lambda\gamma$) in the rest frame of Λ.

In Ref. [26], we define Δ_0 as the phase angle difference between two individual helicity amplitudes, H_{λ_1,λ_2}, for the Λ_c^+ production process $\gamma^* \to \Lambda_c^+(\lambda_1)\bar{\Lambda}_c^-(\lambda_2)$ with total helicities $|\lambda_1 - \lambda_2| = 0$ and 1, respectively. In the case where one-photon exchange dominates the production process, Δ_0 is also the phase between the electric and magnetic form factors of the Λ_c^+ [25,29]. The transverse polarization observable of the produced Λ_c^+ can be defined as

$$\mathcal{P}_T(\cos\theta_0) \equiv \sqrt{1-\alpha_0^2}\cos\theta_0 \sin\theta_0 \sin\Delta_0, \qquad (1)$$

whose magnitude varies as a function of $\cos\theta_0$, and α_0 is the angular distribution parameter of charmed baryon defined by the helicity amplitudes $\alpha_0 = (|H_{1/2,-1/2}|^2 - 2|H_{1/2,1/2}|^2)/(|H_{1/2,-1/2}|^2 + 2|H_{1/2,1/2}|^2)$. Similarly, two parameters, α_{BP}^+ and Δ_1^{BP}, describe the level-1 decays $\Lambda_c^+ \to \Lambda\pi^+$, $\Sigma^+\pi^0$, and $\Sigma^0\pi^+$, where Δ_1^{BP} is the phase angle difference between the two helicity amplitudes in the BP mode. The Lee-Yang parameters [26,30] can be obtained with the relations

$$\beta_{BP} = \sqrt{1-(\alpha_{BP}^+)^2}\sin\Delta_1^{BP},$$
$$\gamma_{BP} = \sqrt{1-(\alpha_{BP}^+)^2}\cos\Delta_1^{BP}. \qquad (2)$$

In the angular analysis, the free parameters describing the angular distributions for the four data sets are determined from a simultaneous unbinned maximum likelihood fit, as α_0 and Δ_0 are common. The likelihood function is constructed from the probability density function (PDF) jointly by

TABLE I. Parameters measured in this analysis.

Parameters	$\Lambda_c^+ \to pK_S^0$	$\Lambda\pi^+$	$\Sigma^+\pi^0$	$\Sigma^0\pi^+$
α_{BP}^+	$0.18 \pm 0.43 \pm 0.14$	$-0.80 \pm 0.11 \pm 0.02$	$-0.57 \pm 0.10 \pm 0.07$	$-0.73 \pm 0.17 \pm 0.07$
α_{BP}^+ (PDG)	⋯	-0.91 ± 0.15	-0.45 ± 0.32	⋯
β_{BP}	⋯	$0.06^{+0.58+0.05}_{-0.47-0.06}$	$-0.66^{+0.46+0.22}_{-0.25-0.02}$	$0.48^{+0.35+0.07}_{-0.57-0.13}$
γ_{BP}	⋯	$-0.60^{+0.96+0.17}_{-0.05-0.03}$	$-0.48^{+0.45+0.21}_{-0.42-0.04}$	$0.49^{+0.35+0.07}_{-0.56-0.12}$
Δ_1^{BP}(rad)	⋯	$3.0 \pm 2.4 \pm 1.0$	$4.1 \pm 1.1 \pm 0.6$	$0.8 \pm 1.2 \pm 0.2$

$$\mathcal{L}_{\rm data} = \prod_{i=1}^{N_{\rm data}} f_S(\vec{\xi}). \quad (3)$$

Here, $f_S(\vec{\xi})$ is the PDF of the signal process, $N_{\rm data}$ is the number of the events in data and i is event index. The signal PDF $f_S(\vec{\xi})$ is formulated as

$$f_S(\vec{\xi}) = \frac{\epsilon(\vec{\xi})|M(\vec{\xi};\vec{\eta})|^2}{\int \epsilon(\vec{\xi})|M(\vec{\xi};\vec{\eta})|^2 {\rm d}\vec{\xi}}, \quad (4)$$

where the variable $\vec{\xi}$ denotes the kinematic angular observables, and $\vec{\eta}$ denotes the free parameters to be determined. $M(\vec{\xi})$ is the total decay amplitude [26] and $\epsilon(\vec{\xi})$ is the detection efficiency parametrized in terms of the kinematic variables $\vec{\xi}$. The background contribution to the joint likelihood is subtracted according to the calculated likelihoods for the type-I background based on inclusive MC simulations and for the type-II background according to the $M_{\rm BC}$ sideband. With a MC sample of sufficiently large size, the integration of the normalization factor is calculated as follows

$$\int \epsilon(\vec{\xi})|M(\vec{\xi};\vec{\eta})|^2 {\rm d}\vec{\xi} = \frac{1}{N_{\rm gen}} \sum_{k_{\rm MC}}^{N_{\rm MC}} |M(\vec{\xi}_k;\vec{\eta})|^2, \quad (5)$$

where $N_{\rm gen}$ is the total number of MC-simulated signal events. $N_{\rm MC}$ is the number of the MC signal events survived from the full selection criteria and $k_{\rm MC}$ is its event index.

Minimization of the negative logarithmic likelihood with background subtraction over all the four signal processes is carried out using the MINUIT package [31]. Here, α_0 is fixed to the known value -0.20 [29]. For the charge-conjugation $\bar{\Lambda}_c^-$ decays, under the assumption of CP conservation, $\bar{\Delta}_0 = \Delta_0$, $\alpha_{BP}^+ = -\alpha_{\bar{B}\bar{P}}^-$, and $\bar{\Delta}_1^{\bar{B}\bar{P}} = -\Delta_1^{BP}$. The decay asymmetry parameter α_Λ for $\Lambda \to p\pi^-$ is taken from the recent BESIII measurement [24] and α_{Σ^+} for $\Sigma^+ \to p\pi^0$ from the Particle Data Group (PDG) [2]. In the fit, the statistical uncertainty of parameters in question is determined by the MINUIT package, which corresponds to the change of one-standard-deviation value of log-likelihood function. From the fit, we obtain $\sin\Delta_0 = -0.28 \pm 0.13({\rm stat.})$ which differs from zero with a statistical significance of 2.1σ according to a likelihood ratio test. This indicates that transverse polarization $\mathcal{P}_T$ of the Λ_c^+ is nonzero when $\sin(2\theta_0) \neq 0$. The numerical fit results are given in Table I, together with the calculated γ_{BP} and β_{BP}.

In Fig. 3, the fit results are illustrated using several projection variables. The data are compared with the MC generated events reweighted according to the fit.

For the $\Lambda_c^+ \to \Lambda\pi^+$ and $\Sigma^+\pi^0$ decays, if all angles are integrated over except for the angle θ_2, the decay rate becomes [32]

$$\frac{dN}{d\cos\theta_2} \propto 1 + \alpha^+_{\Lambda\pi^+(\Sigma^+\pi^0)}\alpha_{\Lambda(\Sigma^+)}\cos\theta_2. \quad (6)$$

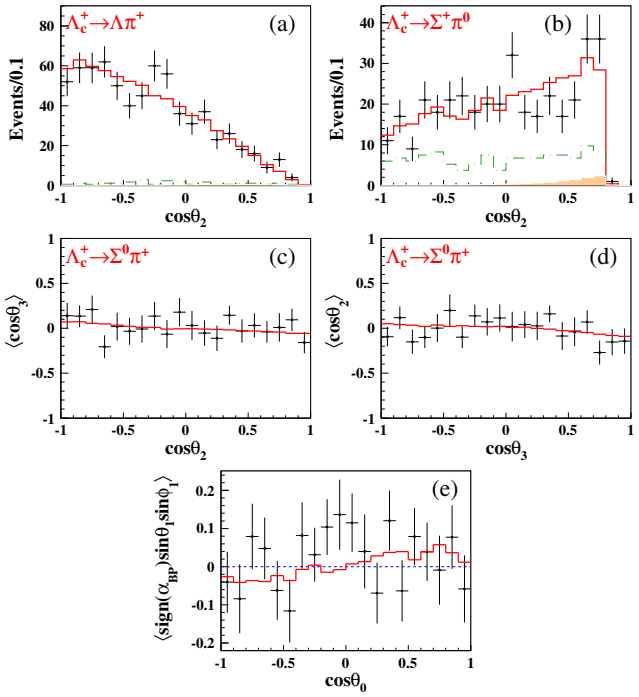

FIG. 3. $\cos\theta_2$ distributions in (a) $\Lambda\pi^+$, and (b) $\Sigma^+\pi^0$; (c) average value of $\cos\theta_3$ as a function of $\cos\theta_2$, and (d) average value of $\cos\theta_2$ as a function of $\cos\theta_3$ in $\Lambda_c^+ \to \Sigma^0\pi^+$; (e) $\langle {\rm sign}(\alpha_{BP})\sin\theta_1\sin\phi_1\rangle$ as a function of $\cos\theta_0$ for all the four signal channels. Points with error bars correspond to data; (red) solid lines represent the MC-determined shapes taking into account the fit results; (green) dash-dotted lines represent the Type-II background and shaded histograms show the type-I background.

Equation (6) shows a characteristically longitudinal polarization of the produced $\Lambda(\Sigma^+)$ from the Λ_c^+ decays, and the asymmetry of $\cos\theta_2$ distribution reflects the product of the decay asymmetries $\alpha^+_{\Lambda\pi^+}\alpha_\Lambda(\alpha^+_{\Sigma^+\pi^0}\alpha_{\Sigma^+})$ [33]. The distributions of $\cos\theta_2$ in the $\Lambda_c^+ \to \Lambda\pi^+$ and $\Sigma^+\pi^0$ modes are shown in Figs. 3(a) and (b), respectively. The drop at the right side in Fig. 3(b) is due to the $K_S^0 \to \pi^0\pi^0$ veto.

For the $\Lambda_c^+ \to \Sigma^0\pi^+$ decay, the correlations of $\cos\theta_2$ and $\cos\theta_3$ in the subsequent level-2 decay $\Sigma^0 \to \gamma\Lambda$ and level-3 decay $\Lambda \to p\pi^-$, are shown in Figs. 3(c) and (d), respectively. The correlation of the average value of $\cos\theta_i$ satisfies the relation

$$\langle\cos\theta_i\rangle = -\frac{1}{6}\alpha^+_{\Sigma^0\pi^+}\alpha_\Lambda\cos\theta_j, \tag{7}$$

with $(i, j) = (2, 3)$ or $(3, 2)$.

If the full expressions for the joint angular distributions (Ref. [26]) are integrated over the angles of the level 2 and 3 decay products, the remaining partial decay rate $\mathcal{W}$ is

$$\mathcal{W} \propto 1 + \alpha_0\cos^2\theta_0 + \mathcal{P}_T\alpha^+_{BP}\sin\theta_1\sin\phi_1. \tag{8}$$

Therefore, in a given $\cos\theta_0$ interval,

$$\langle\sin\theta_1\sin\phi_1\rangle = \frac{\int_0^{2\pi}\int_{-1}^{1}\sin\theta_1\sin\phi_1\mathcal{W}\mathrm{d}\cos\theta_1\mathrm{d}\phi_1}{\int_0^{2\pi}\int_{-1}^{1}\mathcal{W}\mathrm{d}\cos\theta_1\mathrm{d}\phi_1}$$

is directly proportional to $\alpha_{BP}P_T(\cos\theta_0)/(1+\alpha_0\cos^2\theta_0)$ for the acceptance corrected data. In Fig. 3(e), the effect of the transverse polarization $P_T(\cos\theta_0)$ is illustrated by plotting the average value $\langle\mathrm{sign}(\alpha_{BP})\sin\theta_1\sin\phi_1\rangle$ from all four decay modes and including both particles and antiparticles. The sign function of the measured decay asymmetry parameter, $\mathrm{sign}(\alpha_{BP})$, is used to avoid the cancellation of contributions from the opposite charge modes.

IV. SYSTEMATIC UNCERTAINTIES

The systematic uncertainties arise mainly from the reconstruction of final state tracks, $K_S^0 \to \pi^0\pi^0$ veto, ΔE requirement, signal M_{BC} selections and background subtraction. The contributions are summarized in Table II. The uncertainty due to the input α_0 is found to be negligible, after considering the experimental uncertainty [29]. Systematic uncertainties from different sources are combined in quadrature to obtain the total systematic uncertainties.

To understand the reconstruction efficiencies in data and MC simulations, a series of control samples are used for different final states. The proton and charged pion are studied based on the channel $J/\psi \to p\bar{p}\pi^+\pi^-$, photon on $e^+e^- \to \gamma\mu^+\mu^-$ [34], π^0 on $\psi(3686) \to \pi^0\pi^0 J/\psi$ and $e^+e^- \to \omega\pi^0$, Λ on $J/\psi \to \bar{p}K^+\Lambda$ and $J/\psi \to \Lambda\bar{\Lambda}$ [35], and K_S^0 on $J/\psi \to K^*(892)^+K^-$, $K^*(892)^+ \to K_S^0\pi^+$ and $J/\psi \to \phi K_S^0 K^+\pi^-$ [36]. The efficiency differences between data and MC simulations are used to reweight the summed likelihood values. The changes of the fit results after likelihood minimization are taken as systematic uncertainties. The uncertainties due to the $K_S^0 \to \pi^0\pi^0$ veto in $\Sigma^+\pi^0$ candidate events are evaluated by taking the maximum changes with respect to the nominal results when varying the $\pi^0\pi^0$ veto range. A similar method is applied when estimating the systematic uncertainties from the signal ΔE and M_{BC} selection criteria. The background contributions are modeled with the sideband control samples and the inclusive MC samples, and then subtracted from the data likelihood function. The associated uncertainties are studied by varying the sideband range and adjusting the scaling factors of the two background components. The altered scaling factors are obtained by changing the background lineshapes within their 1σ uncertainties from the fits to the M_{BC} distribution. The resultant maximum changes of the fit results are taken as corresponding systematic uncertainties.

V. SUMMARY

To summarize, based on the 567 pb^{-1} data sample collected from e^+e^- collisions at a CM energy of 4.6 GeV, a simultaneous full angular analysis of four decay modes of $\Lambda_c^+ \to pK_S^0$, $\Lambda\pi^+$, $\Sigma^+\pi^0$, and $\Sigma^0\pi^+$ from the $e^+e^- \to \Lambda_c^+\bar{\Lambda}_c^-$ production is carried out. We study the Λ_c^+ transverse polarization in unpolarized e^+e^- collisions for the first time, which gives $\sin\Delta_0 = -0.28 \pm 0.13 \pm 0.03$ with a statistical significance of 2.1σ. This information will help in understanding the production mechanism of the charmed baryons in e^+e^- annihilations. With availability of the transverse polarization measurement, the decay asymmetry parameter in $\Lambda_c^+ \to pK_S^0$ becomes accessible experimentally. Moreover, this improves the precision in

TABLE II. Summary of the systematic uncertainties. A, B, C and D stand for the modes of pK_S^0, $\Lambda\pi^+$, $\Sigma^+\pi^0$, and $\Sigma^0\pi^+$, respectively.

Source	α_A^+	α_B^+	α_C^+	α_D^+	$\sin\Delta_0$	Δ_1^B	Δ_1^C	Δ_1^D
Reconstruction	0.00	0.00	0.00	0.01	0.00	0.8	0.0	0.0
$\pi^0\pi^0$ veto	0.01	0.00	0.01	0.00	0.00	0.0	0.2	0.0
ΔE signal region	0.07	0.01	0.02	0.05	0.02	0.3	0.1	0.1
M_{BC} signal region	0.12	0.01	0.05	0.02	0.02	0.5	0.4	0.1
Background subtraction	0.03	0.01	0.05	0.04	0.02	0.3	0.3	0.0
Total	0.14	0.02	0.07	0.07	0.03	1.0	0.6	0.2

determining the decay asymmetry parameters in $\Lambda_c^+ \to \Lambda\pi^+$, $\Sigma^+\pi^0$, and $\Sigma^0\pi^+$, as listed in Table I.

The parameters $\alpha^+_{pK^0_S}$ and $\alpha^+_{\Sigma^0\pi^+}$ are measured for the first time. The measured $\alpha^+_{\Lambda\pi^+}$ and $\alpha^+_{\Sigma^+\pi^0}$ parameters are consistent with previous measurements, but with much improved precisions (by a factor of 3 for $\alpha^+_{\Sigma^+\pi^0}$). The negative sign of the $\alpha^+_{\Sigma^+\pi^0}$ parameter is confirmed and differs from the positive predictions [10–15] by at least 8σ, which rules out those model calculations. The measured $\alpha^+_{\Sigma^+\pi^0}$ and $\alpha^+_{\Sigma^0\pi^+}$ values agree well, which supports hyperon isospin symmetry in Λ_c^+ decay. For the results on $\alpha^+_{pK^0_S}$, $\alpha^+_{\Sigma^+\pi^0}$, and $\alpha^+_{\Sigma^0\pi^+}$ listed in Table I, at present no model gives predictions fully consistent with all the measurements. These improved results in Λ_c^+ decay asymmetries provide essential inputs for the b-baryon decay asymmetry measurements to be performed in the future.

ACKNOWLEDGMENTS

The BESIII collaboration thanks the staff of BEPCII and the IHEP computing center for their strong support. This work is supported in part by National Key Basic Research Program of China under Contract No. 2015CB856700; National Natural Science Foundation of China (NSFC) under Contracts No. 11335008, No. 11425524, No. 11625523, No. 11635010, No. 11735014; the Chinese Academy of Sciences (CAS) Large-Scale Scientific Facility Program; the CAS Center for Excellence in Particle Physics (CCEPP); Joint Large-Scale Scientific Facility Funds of the NSFC and CAS under Contracts No. U1532257, No. U1532258, No. U1732263; CAS Key Research Program of Frontier Sciences under Contracts No. QYZDJ-SSW-SLH003, No. QYZDJ-SSW-SLH040; 100 Talents Program of CAS; INPAC and Shanghai Key Laboratory for Particle Physics and Cosmology; German Research Foundation DFG under Contract No. Collaborative Research Center CRC 1044, FOR 2359; Istituto Nazionale di Fisica Nucleare, Italy; Koninklijke Nederlandse Akademie van Wetenschappen (KNAW) under Contract No. 530-4CDP03; Ministry of Development of Turkey under Contract No. DPT2006K-120470; National Science and Technology fund; The Swedish Research Council; U.S. Department of Energy under Contracts No. DE-FG02-05ER41374, No. DE-SC-0010118, No. DE-SC-0012069; University of Groningen (RuG); Helmholtzzentrum fuer Schwerionenforschung GmbH (GSI), Darmstadt; the Knut and Alice Wallenberg Foundation (Sweden) under Contract No. 2016.0157 and the Royal Society, UK under Contract No. DH160214.

[1] Y. Amhis *et al.* (HFLAV Collaboration), Eur. Phys. J. C **77**, 895 (2017).
[2] M. Tanabashi *et al.* (Particle Data Group), Phys. Rev. D **98**, 030001 (2018).
[3] C. D. Lü, W. Wang, and F. S. Yu, Phys. Rev. D **93**, 056008 (2016).
[4] C. Q. Geng, Y. K. Hsiao, C. W. Liu, and T. H. Tsai, J. High Energy Phys. 11 (2017) 147.
[5] F. S. Yu, H. Y. Jiang, R. H. Li, and C. D. Lü, W. Wang, and Z. X. Zhao, Chin. Phys. C **42**, 051001 (2018).
[6] R. Aaij *et al.* (LHCb Collaboration), Phys. Rev. Lett. **119**, 112001 (2017).
[7] H. Y. Cheng, Front. Phys. **10**, 101406 (2015).
[8] M. J. Savage and R. P. Springer, Phys. Rev. D **42**, 1527 (1990).
[9] J. D. Bjorken, Phys. Rev. D **40**, 1513 (1989).
[10] H. Y. Cheng and B. Tseng, Phys. Rev. D **48**, 4188 (1993).
[11] Q. P. Xu and A. N. Kamal, Phys. Rev. D **46**, 270 (1992).
[12] J. G. Korner and M. Kramer, Z. Phys. C **55**, 659 (1992).
[13] H. Y. Cheng and B. Tseng, Phys. Rev. D **46**, 1042 (1992); **55**, 1697(E) (1997).
[14] M. A. Ivanov, J. G. Korner, V. E. Lyubovitskij, and A. G. Rusetsky, Phys. Rev. D **57**, 5632 (1998).
[15] P. Zenczykowski, Phys. Rev. D **50**, 5787 (1994).
[16] K. K. Sharma and R. C. Verma, Eur. Phys. J. C **7**, 217 (1999).
[17] P. Zenczykowski, Phys. Rev. D **50**, 402 (1994).
[18] A. Datta, arXiv:hep-ph/9504428.
[19] J. M. Link *et al.* (FOCUS Collaboration), Phys. Lett. B **634**, 165 (2006).
[20] M. Bishai *et al.* (CLEO Collaboration), Phys. Lett. B **350**, 256 (1995).
[21] H. Albrecht *et al.* (ARGUS Collaboration), Phys. Lett. B **274**, 239 (1992).
[22] P. Avery *et al.* (CLEO Collaboration), Phys. Rev. Lett. **65**, 2842 (1990).
[23] Y. Guan *et al.* (Belle Collaboration), Phys. Rev. Lett. **122**, 042001 (2019).
[24] M. Ablikim *et al.* (BESIII Collaboration), Nat. Phys. **15**, 631 (2019).
[25] G. Fäldt, Phys. Rev. D **97**, 053002 (2018).
[26] See Supplemental Material at http://link.aps.org/supplemental/10.1103/PhysRevD.100.072004 for the joint angular formula and Lee-Yang parameters.
[27] M. Ablikim *et al.* (BESIII Collaboration), Phys. Rev. Lett. **116**, 052001 (2016).
[28] H. Albrecht *et al.* (ARGUS Collaboration), Phys. Lett. B **241**, 278 (1990).

[29] M. Ablikim *et al.* (BESIII Collaboration), Phys. Rev. Lett. **120**, 132001 (2018).
[30] T. D. Lee and C. N. Yang, Phys. Rev. **108**, 1645 (1957).
[31] F. James and M. Roos, Comput. Phys. Commun. **10**, 343 (1975).
[32] D. Wang, R.-G. Ping, L. Li, X.-R. Lyu, and Y.-H. Zheng, Chin. Phys. C **41**, 023106 (2017).
[33] D. M. Asner *et al.*, Int. J. Mod. Phys. A **24**, S1 (2009).
[34] V. Prasad, C. Liu, X. Ji, W. Li, H. Liu, and X. Lou, Springer Proc. Phys. **174**, 577 (2016).
[35] M. Ablikim *et al.* (BESIII Collaboration), Phys. Rev. Lett. **121**, 062003 (2018).
[36] M. Ablikim *et al.* (BESIII Collaboration), Phys. Rev. D **92**, 112008 (2015).